CLM - P 152

CLM - P 152

United Kingdom Atomic Energy Authority
RESEARCH GROUP
Preprint

AREA WAVES IN A THETA PINCH

A. A. NEWTON

Culham Laboratory
Abingdon Berkshire

1967

UNCLASSIFIED
(Approved for Publication)

CLM -P 152

AREA WAVES IN A THETA PINCH

by

A.A. NEWTON

(Submitted for publication in Nuclear Fusion)

ABSTRACT

Measurements made in the mid-plane of a theta pinch plasma indicate a sudden decrease in line density. This is interpreted as the arrival of a rarefaction wave due to axial plasma loss. Detailed predictions of density, and β given by an axial MHD computation, are in good agreement with the observations.

U.K.A.E.A. Research Group,
Culham Laboratory,
Abingdon,
Berks.

October, 1967 (MEJ)

CONTENTS

1. INTRODUCTION

When a plasma is compressed and heated by the magnetic field of a single turn coil of finite length, the plasma is expected to flow parallel to the field lines to regions out of the ends of the coil. If the plasma pressure is comparable with the magnetic pressure this flow is marked by a decrease in the plasma cross-section area. The decrease occurs initially at the ends and travels towards the mid-plane. This effect is known as a rarefaction wave.

The theory of plasma flow in the theta pinch has been given by Taylor and Wesson(1). The time variation of magnetic field was included in a later model by Wesson(2). A more complete description of the plasma behaviour including thermal losses can be obtained with a numerical computation(3).

In this paper the existence of a rarefaction wave is inferred from the occurrence of an abrupt change in line density in the mid-plane of a theta pinch. Observations of line density, density and β agree with the predictions of the Fisher and Roberts model.

2. APPARATUS

A megajoule capacitor bank(4) was used to feed a one metre long coil 19 cm in diameter and when discharged at 30 kV generated peak field of 45 kG at 10 μsec. The quartz vacuum vessel was 16 cm bore in a central region 75 cm long and the ends were reduced to 8 cm bore. The enlarged portion was positioned symmetrically under the coil. Deuterium at 14 mtorr was preionized with a 40 kV, 1Ω artificial transmission line(5,6).

3. MEASUREMENT OF LINE DENSITY

Measurements of luminosity across the plasma diameter as a function of time have been made with a calibrated streak camera(7) of the image convertor type. Relative values of the radial distribution of electron density, $n_e(r)$, were obtained assuming the radiation to have the intensity, I, of bremsstrahlung

$$I = kn_e^2\, T_e^{-\frac{1}{2}} \qquad \ldots (1)$$

and using Abel's inversion. Densities determined in this way are weakly dependent on the electron temperature, T_e, so that variations in T_e were neglected.

Spectroscopic studies showed that after the implosion phase, light from the plasma was continuum radiation, justifying the use of equation (1). A faint, uniform background illumination, consisting of oxygen and silicon lines, was observed to originate from fluorescence of the tube walls outside the confines of the coil. In the analysis this residual intensity was identified by its uniformity and subtracted from the total intensity.

A streak photograph of the plasma in the coil mid-plane is shown in Fig.1. Shot to shot reproducibility was good.

The magnetic flux, S, displaced by the plasma was measured by the technique of balanced double loops(8). A tracing of S in the mid-plane is shown in Fig.2. From the frequency of the radial hydromagnetic oscillations(9,10) the plasma line density was estimated to be $N = 1{\cdot}6 \times 10^{17}\ \text{cm}^{-1}$. Since $N = 2\pi \int n_e(r)dr$ the above value was taken to establish an absolute density scale at 2·8 μsec.

Radial distributions of electron density observed in the mid-plane are shown in Fig.3. The shape of the distribution is similar to that observed by Bodin et al.$^{(5)}$.

The tendency of density on axis to increase with time is due to a rise of the confining magnetic field. There is a corresponding decrease in radius. However, the maximum density is reached before peak magnetic field and fluctuations in the plasma radius can be seen.

The line density is shown in Fig.3 where increases of 30% and 15% can be seen at 3·5 and 4·8 μsec. The occurrence of these was simultaneous with increases in the plasma radius and small humps in the diamagnetism. After a plateau between 5·3 and 6·2 μsec N fell to 40% of its initial value by 8·5 μsec.

4. INTERPRETATION OF THE RESULTS

The disturbances in line density are interpreted as area waves propagating from the ends of the plasma. These were formed at the constrictions in the tube where its area changed by a factor of four. Thus the effective length of the plasma was 75 cm. To calculate mean speeds of the waves they were assumed to start at a time intermediate between the radial implosion times observed in the wide and narrow regions i.e. 0·6 μsec.

After 6·2 μsec the fall in line density is caused by a rarefaction wave having a front speed of 6·7 cm/μsec. This is preceded by a rise in line density at 3·5 μsec due to a compression wave with a speed of 13 cm/μsec. At 4·8 μsec a second lower amplitude increase is seen. From its arrival time this may be either a wave with a speed of 9 cm/μsec or a reflection of the first compression off the rarefaction front. Trajectories of the wave fronts are shown in Fig.5.

5. DISCUSSION

(a) Temperatures and Beta

Theories of wave propagation give velocities in terms of the plasma sound speed and β. These may be estimated from the measured density and diamagnetism in the following way.

Mean values of beta, $\bar{\beta}$ and temperature, $\bar{T} = (\overline{T_e + T_i})$, assuming radially uniform temperatures and densities and no rotation, are defined by pressure balance,

$$16 \pi k \, n(o)\bar{T} = \bar{\beta} B^2 \qquad \ldots (2)$$

and diamagnetism (e.g. see ref.3)

$$16 \pi k \, N \bar{T} = SB \, (1 + \sqrt{1 - \bar{\beta}}) \qquad \ldots (3)$$

$n(o)$ is the density on axis and B the magnetic field at the tube wall. Solution of these simultaneous equations gave $\bar{T}$ equal to 225, 190 and 175 eV at 2·8, 5·7 and 9·2 μsec respectively. Corresponding values of $\bar{\beta}$ were 0·9, 0·8 and 0·5. The errors in $\bar{\beta}$ and $\bar{T}$ were estimated to be ± 15% and ± 20%.

The temperatures show the limitation observed in previous experiments attributed to axial thermal conduction(3). Scaling the limiting temperature to the present experiment one would expect $T_e \leqslant 130 \pm 30$ eV which is consistent with the observed $\bar{T}$, preferential ion heating in the implosion and the estimated ion-electron thermalisation time.

Thus the temperature varies slowly having a mean value ~ 400 eV and the plasma sound speed, $C_s = (\gamma k 2\bar{T}/m_i)^{\frac{1}{2}}$ can be taken as 18 cm/μsec and approximately constant.

(b) Rarefaction Wave

Wesson(2), using a radially uniform plasma model, derived an expression for the rarefaction wave speed in terms of the plasma β,

$$V = (\frac{2}{\gamma})^{\frac{1}{2}} (1 - \beta)^{\frac{1}{2}} C_s \qquad \ldots (4)$$

Agreement with the observed velocity and the estimated sound speed is obtained with $\beta = 0{\cdot}88$ which is close to the experimental $\bar{\beta}$.

Since β varies with time the MHD code of Fisher and Roberts(3) is used to calculate the arrival time of the wave in the mid-plane. This code has been obtained by changing the co-ordinates of the radial code(10) and eliminating the cylindrical effects. The plasma is treated as a radially uniform cylinder with trapped flux conserved. Axial variations of density, temperature and velocity are calculated taking into account the flow of plasma and heat.

Computations have been made with four initial values of β (i.e., β_o) at some arbitrary early time. Other initial conditions were taken from the measured plasma properties. Fig.6 shows the computed and measured line densities. Best agreement with the timing and shape of the rarefaction feature is given by $\beta_o = 0{\cdot}95$. In the computation, the wave front arrives later as β_o is increased, in accord with equation (4). Fig.7 shows the computed densities compared with the measured n(o). The nearly linear rise of density is different from that which would be expected in an adiabatic compression with no energy loss and tends towards the form expected with an isothermal compression. The density maximum occurs during the particle loss phase just before the internal magnetic flux begins to make the dominant contribution to pressure balance.

Since the wave velocity depends on β it is instructive to compare the computed β with the measured $\bar{\beta}$. In Fig.8 it can be seen that β falls slowly until the rarefaction wave reaches the mid-plane. After the rarefaction, the decline in β is rapid. Again best agreement between computation and experiment is obtained with $\beta_o = 0{\cdot}95$ and its mean value up to 6·2 μsec is close to that obtained using equation (4).

(c) Compression Wave

The properties of area waves and shocks, including compression waves, propagating along a uniform plasma column in a steady magnetic field have been analysed by Taylor(12) who showed that the wave speed depended on its amplitude, β and the degree of compression Z, (where Z is the ratio of coil to plasma area). For small amplitude waves with $Z > 10$

$$\frac{C_s^2}{V^2} = 1 + \frac{\gamma\,\beta\,(1 + Z)}{2[\beta + (1 - \beta)Z]} \qquad \ldots (5)$$

All quantities in equation (5) vary with time in the early discharge so that accurate comparison with the compression wave properties is of limited value. However, when $Z \approx 10$ agreement is obtained with $\beta \approx 0{\cdot}6$, suggesting that the compression wave propagates in the outer regions of the plasma. In an ancillary experiment a magnetic mirror ratio of 1·5 was applied. The line density doubled at 4 μsec showing that the compression wave had substantially the same velocity and confirmed that radial components of field, produced either by the tube discontinuity or by the mirrors, initiated the compression wave.

6. CONCLUSION

An abrupt fall in the line density has been observed to occur in the mid-plane of a theta pinch. The decrease is interpreted as the arrival of the rarefaction wave due to axial particles loss. The plasma behaviour has been compared with a numerical model which assumes a radially uniform distribution of density in the plasma. Agreement was obtained between the measured line density, density on axis and mean beta and the predictions of the model. The plasma density varies with radius and at the boundary where β is low the plasma loss will occur sooner and be more rapid than on axis. Nevertheless the model appears to give good agreement with the observations.

7. ACKNOWLEDGEMENTS

The author is grateful to J.A. Wesson and H.A.B. Bodin for discussions. Thanks are also due to I.K. Pasco who processed the photographic data, and to T. Quayle and his staff for the operation of the capacitor bank.

8. REFERENCES

1. TAYLOR, J.B. and WESSON, J.A. Nucl. Fusion 5 (1965) 159.

2. WESSON, J.A. Proc. Conf. on Plasma Physics and Controlled Fusion Research, Culham, 1965. IAEA, Vienna, 1 (1966) 223.

3. GREEN, T.S. et al. Phys. Fluids 10 (1967) 1663.

4. McCORMICK, N.R. A one-megajoule low-inductance capacitor bank for nuclear fusion research. Culham Laboratory, 1967. CLM - P 130.

5. BODIN, H.A.B. et al. Proc. Conf. on Plasma Physics and Controlled Fusion Research, Culham, 1965. IAEA, Vienna, 1 (1966) 193.

6. NEWTON, A.A. Fast high voltage Z-preionization of a megajoule theta pinch. Culham Laboratory, 1966. CLM - R 62.

7. KOLB, A.C. et al. Proc. Conf. on Plasma Physics and Controlled Fusion Research, Culham, 1965. IAEA, Vienna, 1 (1966) 261.

8. GREEN, T.S. Nuclear Fusion 3 (1963) 57.

9. NIBLETT, G.B.F. and GREEN, T.S. Proc. Phys. Soc. 74 (1959) 737.

10. BODIN, H.A.B. and McNAMARA, B. Radial oscillations of a plasma cylinder with arbitrary density distribution. Culham Laboratory, 1966. CLM - P 117.

11. HAIN, K. et al. Z. fur Naturf. 15a, (1960) 1039.

12. TAYLOR, J.B. see appendix to BODIN, H.A.B. et al. Nuclear Fusion, 1962, Part 2, 511.

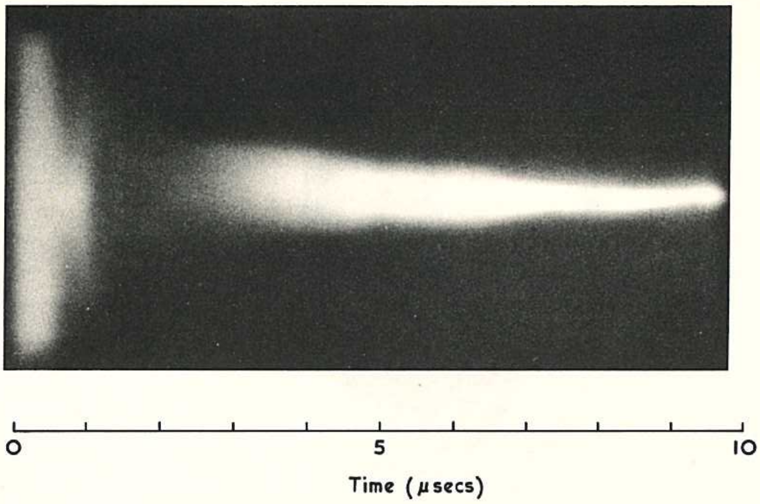

Fig. 1 (CLM-P 152)
Streak photograph of deuterium plasma taken in the mid-plane of the coil

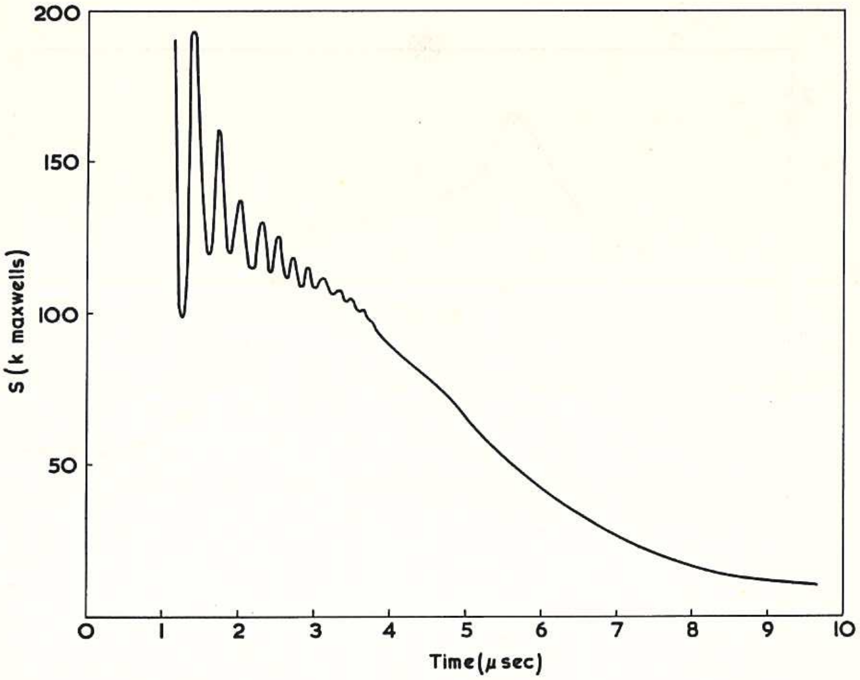

Fig. 2 Plasma diamagnetism (CLM-P 152)

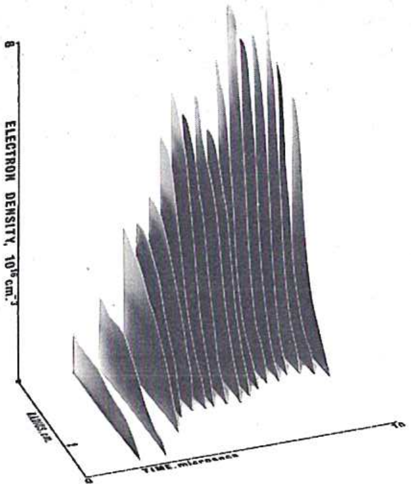

Fig. 3 Measured radial electron density distributions (CLM-P 152)

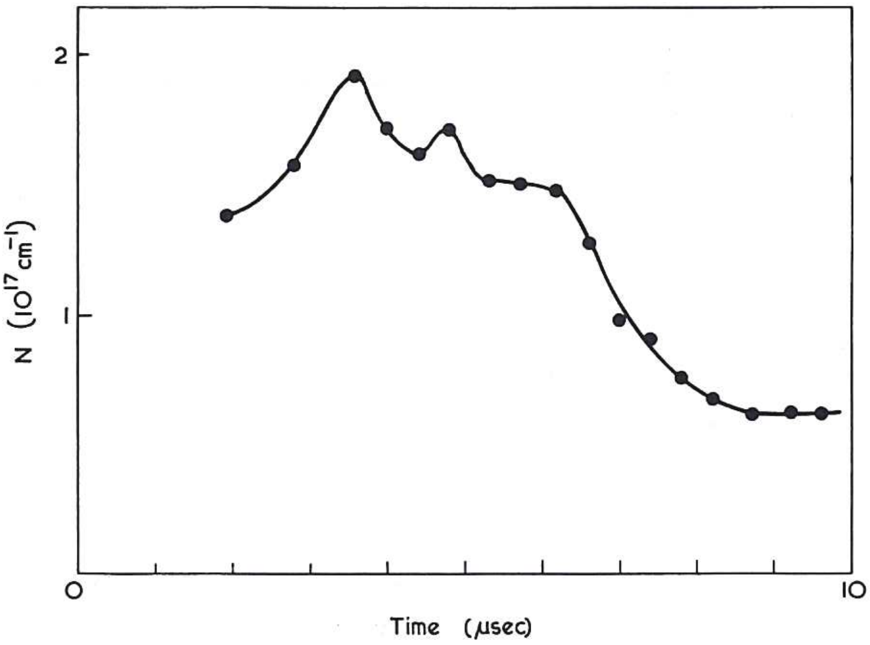

Fig. 4 Line density as a function of time (CLM-P 152)

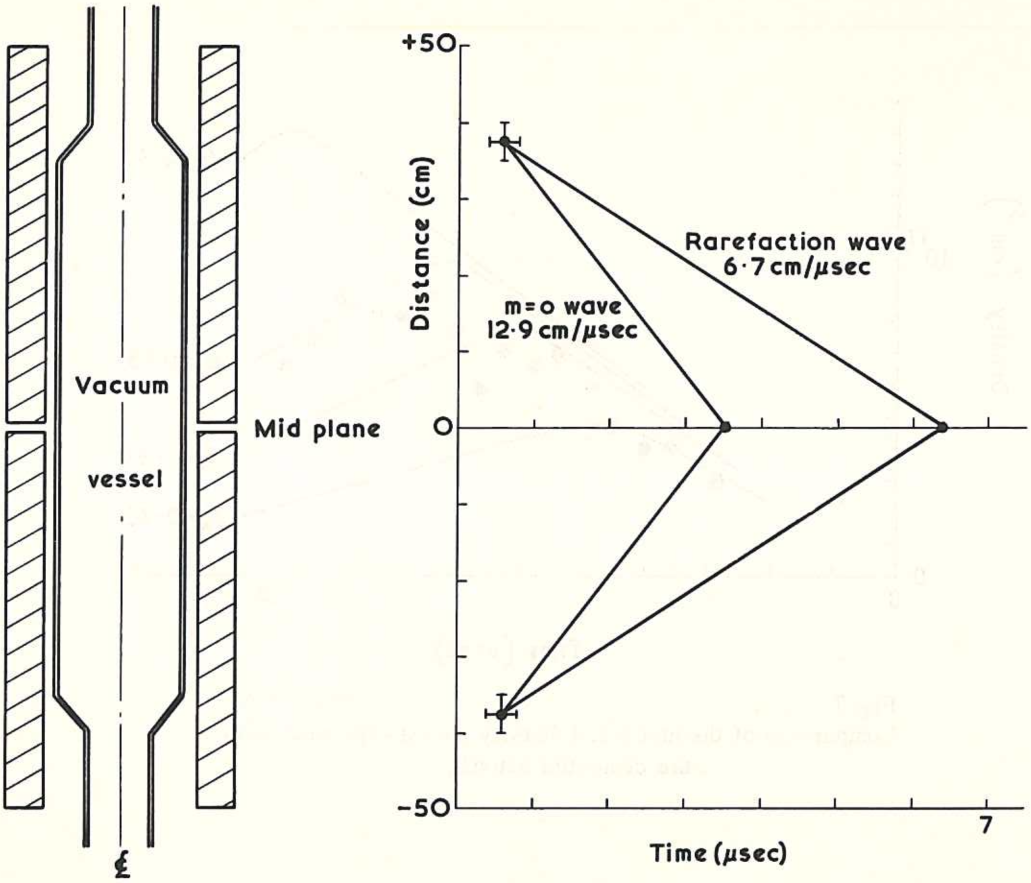

Fig. 5 Interpretation of waves propagating along the plasma column (CLM-P 152)

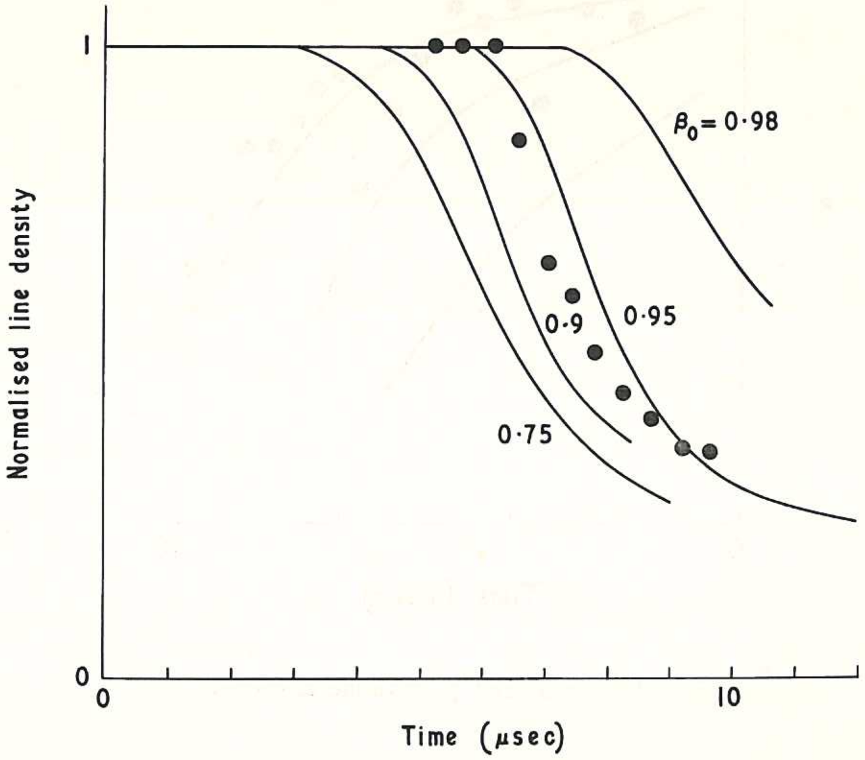

Fig. 6 (CLM-P 152)
Comparison of the measured line density (points) with the computation using various initial values of β i.e., β_0.

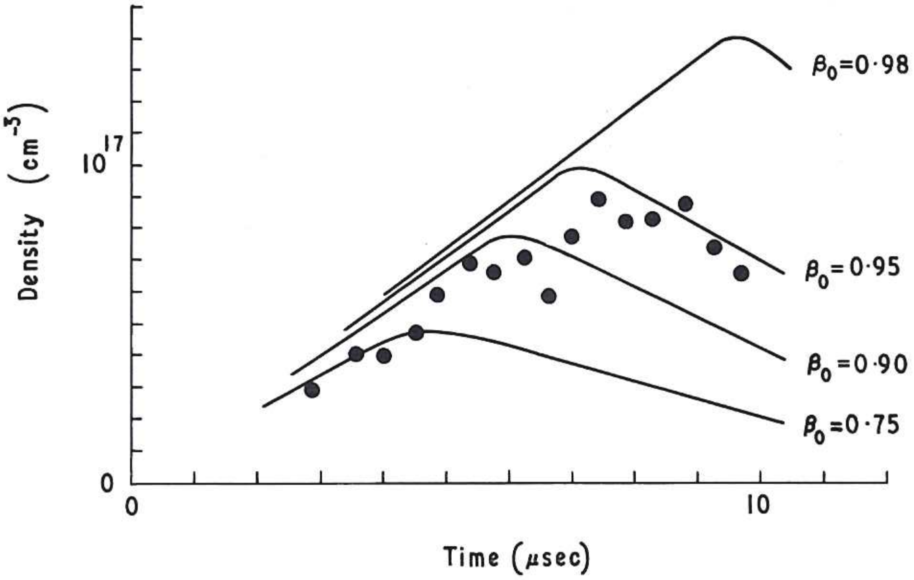

Fig. 7 (CLM-P 152)
Comparison of the measured density on axis (points) with the computed density.

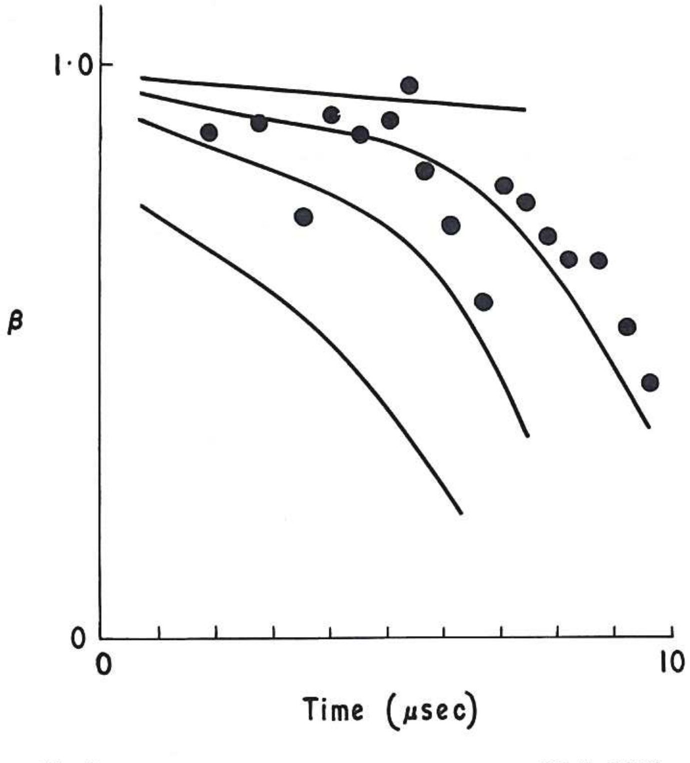

Fig. 8 (CLM-P 152)
Comparison of the measured β with the computed β